

Development of Hydrogen Separation Ceramics Membranes for Ultra Pure Hydrogen Production and Evaluation of Their Transport Properties

超高純度水素製造のための水素分離セラミクス膜の開発と輸送特性評価

Atsushi Unemoto, Assistant Professor, Institute of Multidisciplinary Research for Advanced
Materials, Tohoku University

1. Introduction

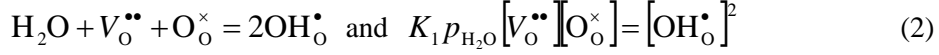
Hydrogen enables us to generate electricity cleanly by the combination with polymer electrolyte fuel cells (PEFCs). Thus, hydrogen is considered as an energy carrier to the next generation. However, CO poisoning on Pt electro-catalysts of PEFC invites a serious irreversible degradation of the electricity generation performance. Thus, ultra pure hydrogen with CO concentrations below 10 ppm is requested.

Possible hydrogen sources are such as the waste gas, *e.g.* coke oven gas (COG) *etc.* and reformed gas of methane and methanol. In these cases, hydrogen needs to be recovered selectively from the gas mixtures. Pressure swing adsorption (PSA) method is employed conventionally for the above purpose. On the other hand, hydrogen separation membranes allow simplified and compact system because those purify hydrogen in only one step. In order to make use of this advantage, hydrogen separation membrane with a cost effective materials and high stability at higher temperatures is one of the important technological challenges to realize commercial use of the system because it directly determines the hydrogen production/recovery efficiencies.

This study aims to develop ceramic membranes based on the protonic conductors, which pumps hydrogen by the current flow via the external circuit. This is because a class of the membranes possibly meets the above requirements for hydrogen separation. In the case of high-temperature proton conducting zirconates, the interstitial protonic defects contribute to the protonic conductivity. Substitution of lower valent cation into the Zr-site leads to the formation of oxygen vacancy. For example, the reaction between SrZrO₃ with the metal oxides having lower valent cation than Zr-ion such as M₂O₃ is expressed as,



where Kröger – Vink notation [1] was employed to express the defects. M'_{Zr} , O^{\times}_O and $V^{\bullet\bullet}_O$ are M^{3+} -ion in Zr-site, oxide-ion in their site and oxygen vacancy, respectively. Then, the oxygen vacancy accepts ambient water vapor, which leads to the formation of protonic defects as,



where OH^{\bullet}_O and K_1 represents protonic defect and the equilibrium constant.

Since the first discovery of high temperature proton conducting cerates, $Sr(Ce,Y)O_3$, by Iwahara *et al.* [2], the protonic conductivities of rare earth doped zirconates have been investigated so far because zirconates have superior stability to cerates against carbon dioxide and water vapor [3]. However, the ceramics suffer from the insufficient protonic conductivities. In this study, we chose the pseudo-ternary system, $LaFeO_3 - SrFeO_{3-\delta} - SrZrO_3$. In a reducing environment, the concentration of protonic defects is expected to increase by the increase of oxygen vacancy concentration accompanied by the partial reduction of Fe-ion. To date, formation diagrams [4] and electrical conductivity [4-6] were investigated. However, the knowledge on the conductivity is limited to comparatively higher temperatures such as above 1273 K, where the concentration of protonic defect is expected to be small due to the desorption of water vapor from the ceramics.

In this study, the electrical conductivities of $\{La_{0.05(1-x)}Sr_{0.95+0.05x}\}(Zr_{0.95}Fe_{0.05})O_{3-\delta}$ [or $(La_{1-x}Sr_xFeO_{3-\delta})_{0.05}(SrZrO_3)_{0.95}$] ($x = 0, 0.1, 0.25$ and 0.5) was evaluated at temperatures below 1273 K. Electromotive force (EMF) measurements of hydrogen concentration cells in humidified hydrogen were carried out to investigate the transport number of ionic species. X-ray absorption spectroscopic (XAS) measurements were conducted to investigate the oxidation state of Fe in the oxide.

2. Experimental

Powders of $\{La_{0.05(1-x)}Sr_{0.95+0.05x}\}(Zr_{0.95}Fe_{0.05})O_{3-\delta}$ ($x = 0, 0.1, 0.25$ and 0.5) were prepared by a conventional solid state reaction route. The starting powders, La_2O_3 (99.99 %, Rare Metallic Co., Ltd.), $SrCO_3$ (99.99 %, Rare Metallic Co., Ltd.) and Fe_2O_3 (99.99 %, Kojundo Chemical Laboratory Co., Ltd.) and ZrO_2 (TZ-0, Tosoh Corp.), were precisely weighed in appropriate ratios and mixed in a zirconia mortar with a zirconia pestle in ethanol. The mixtures were then calcined at 1473 – 1623 K for 5 – 10 hours in air. The calcined powders

were crushed in a planetary ball mill (Frisch, P-7) at 300 rpm for 3 hours. The calcination and the crushing were repeated three times. X-ray diffraction (XRD, Bruker AXS, M18X-CE) measurements were conducted to determine if the resultant products of the solid state reaction were a single phase. After sieving, the powders were formed into disks, hydrostatically pressed at 200 MPa, and sintered at 1873 – 2023 K for 5 hours for the electrical conductivity measurements.

Platinum paste was painted on both surfaces of the disks as electrodes for the electrical conductivity measurements with a two-probe ac technique in hydrogen and oxygen containing environments. In order to identify if the proton is a carrier, the isotope effect of hydrogen and deuterium on the electrical conductivity was examined. The individual disk was connected to the sets of and electroanalytical systems consisting of Electrochemical Interface SI1287 and Impedance/Gain-Phase Analyzer SI1260 (Solartron Analytical). EMF (electron motive force) measurements of hydrogen concentration cells under constant partial pressure of water vapor were carried out to determine the transport number of ionic species.

The oxidation states of the transition metal, Fe, of the specimens were investigated by X-ray absorption spectroscopic (XAS) measurements. The powder of the $\{\text{La}_{0.045}\text{Sr}_{0.955}\}(\text{Zr}_{0.95}\text{Fe}_{0.05})\text{O}_{3-\delta}$ was annealed in $\log(p_{\text{O}_2} / \text{atm}) = -0.68$ (in air), -15.73 (in 1.0% H_2 – 1.9% H_2O) and -19.73 (in 1.0% H_2 – 1.9% H_2O) at 1173 K for 5 hours, then, quenched to room temperature. The powders were mixed with boron nitride (BN, > 99 %, Kojundo Chemical Laboratory Co., Ltd.) and then pressed into disks. A pressed body of a mixture of Fe_2O_3 and BN was also prepared as a reference. Spectra of the X-ray absorption near-edge structure (XANES) of Fe K-edge were collected via a transmission mode at the beam line, BL-7C, of the synchrotron radiation facility, Photon Factory (High Energy Accelerator Research Organization, Institute of Materials Structure Science of Japan).

3. Results and Discussion

3.1 Specimens

XRD patterns of the resultant powders and the annealed powders in hydrogen containing environments well matched with the patterns of the literature of SrZrO_3 with an orthorhombic structure [7]. No extra peak was observed for all powders. This suggests that the powders for the following measurements surely consisted of a single phase.

3.2 Electrical conductivity in oxygen

Figure 1 (a) shows the $\{\text{La}_{0.05(1-x)}\text{Sr}_{0.95+0.05x}\}(\text{Zr}_{0.95}\text{Fe}_{0.05})\text{O}_{3-\delta}$ ($x = 0, 0.1, 0.25$ and 0.5) in unhumidified 1.0% O_2 , 1.0% $\text{O}_2 - 1.9\%\text{H}_2\text{O}$ and 1.0% $\text{O}_2 - 1.9\%\text{D}_2\text{O}$ as a function of inverse temperature. For $x = 0.1, 0.25$ and 0.5 , the electrical conductivities exhibit higher values than non-doped SrZrO_3 [4, 6]. This suggests that the electrical conductivity is surely enhanced by co-doping of La and Fe in the Sr-site and Zr-site, respectively. However, the electrical conductivity for $x = 0$ was slightly smaller than that of non-doped SrZrO_3 obtained in air [4, 6]. This may be caused by p -type conduction in which the defect may be induced by the different valence cation impurity [6].

Differences between the electrical conductivities in unhumidified 1.0% O_2 and those in 1.0% $\text{O}_2 - 1.9\%\text{H}_2\text{O}$ were not remarkable for $x = 0$ and 0.1 in the entire temperature ranges and for $x = 0.25$ at higher temperatures. The electrical conductivity in humidified oxygen was higher for $x = 0.25$ at lower temperatures and $x = 0.5$ than those in unhumidified oxygen. In order to determine if proton conductivity contributes to the total in the oxides for $x = 0.25$ and 0.5 , the isotope effects of hydrogen and deuteron on the electrical conductivities were examined. Figure 1 (b) shows the ratio of the electrical conductivities obtained in 1.0% $\text{O}_2 - 1.9\%\text{H}_2\text{O}$ and that in 1.0% $\text{O}_2 - 1.9\%\text{D}_2\text{O}$. As expected in the case which the contribution of protonic conduction is significant, a remarkable isotope effect was observed for $x = 0.5$ at entire temperatures and slightly for $x = 0.25$ at lower temperatures below 973 K. It was found that the difference between the electrical conductivities in 1.0% $\text{O}_2 - 1.9\%\text{H}_2\text{O}$ and 1.0% $\text{O}_2 - 1.9\%\text{D}_2\text{O}$ is $1.77 - 1.03$ at $1223 - 622$ K for $x = 0.5$. At temperatures below 873 K, the ratio exceeded $\sqrt{2}$, which is expected by the classical theory

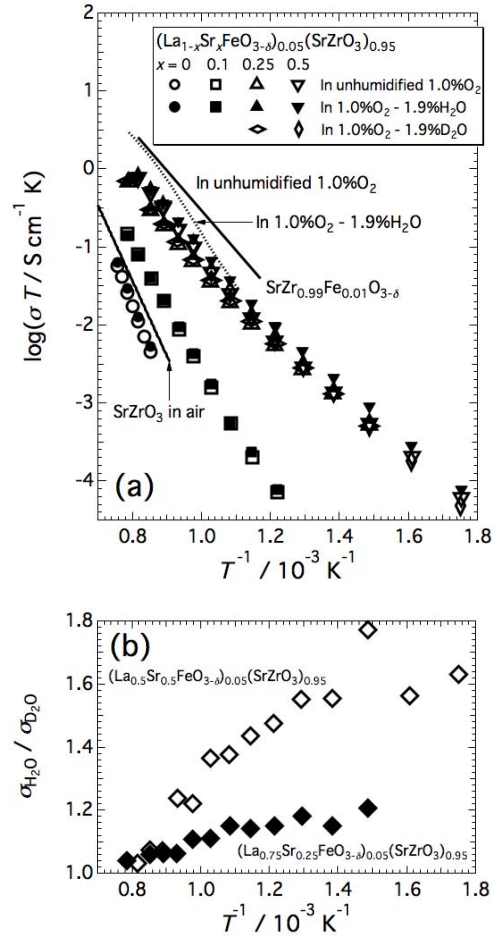
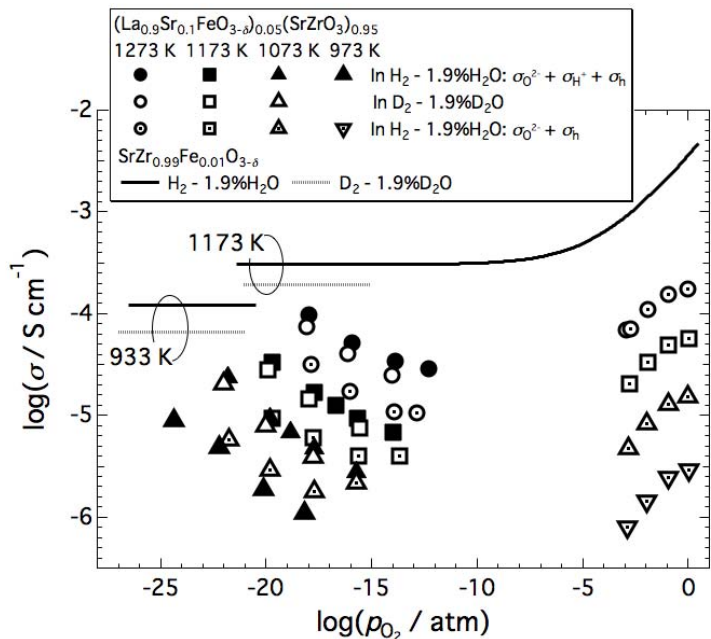


Fig. 1 (a) Electrical conductivities of $\{\text{La}_{0.05(1-x)}\text{Sr}_{0.95+0.05x}\}(\text{Zr}_{0.95}\text{Fe}_{0.05})\text{O}_{3-\delta}$ ($x = 0, 0.1, 0.25$ and 0.5), $\text{SrZr}_{0.99}\text{Fe}_{0.01}\text{O}_{3-\delta}$ [9] and $\text{SrZr}_{0.9}\text{Y}_{0.1}\text{O}_{3-\delta}$ [12]. (b) Isotope effect of H/D for $x = 0.25$ and 0.5 as functions of inverse temperature.

[8]. A possible explanation is because of the difference of zero-point energy, namely, semi-classical theory, which resulted in the difference in activation energies [8]. In the case of $(\text{La}_{0.5}\text{Sr}_{0.5}\text{FeO}_{3-\delta})_{0.05}(\text{SrZrO}_3)_{0.95}$, the activation energies of protonic and deuteron ion conduction are 0.79 and 0.82 eV, respectively. This difference, 0.30 eV, is in the range of the expected value by semi-classical theory. This suggests that proton is carrier for x is above 0.25 in oxygen containing environment.

3.3 Electrical conductivity of $(\text{La}_{0.045}\text{Sr}_{0.955})(\text{Zr}_{0.95}\text{Fe}_{0.05})\text{O}_{3-\delta}$ as a function of oxygen partial pressure

Figure 2 shows the electrical conductivities of $(\text{La}_{0.045}\text{Sr}_{0.955})(\text{Zr}_{0.95}\text{Fe}_{0.05})\text{O}_{3-\delta}$ ($x = 0.1$) and $\text{SrZr}_{0.99}\text{Fe}_{0.01}\text{O}_{3-\delta}$ [9] as a function of oxygen partial pressure in $\text{H}_2 - 1.9\%\text{H}_2\text{O}$, in $\text{D}_2 - 1.9\%\text{D}_2\text{O}$ and in $\text{O}_2 - 1.9\%\text{H}_2\text{O}$ at 973 – 1273 K. For $(\text{La}_{0.075}\text{Sr}_{0.925})(\text{Zr}_{0.9}\text{Fe}_{0.1})\text{O}_{3-\delta}$ ($x = 0.25$), the electrical conductivity degraded gradually in humidified hydrogen. Phase separation might occur with the reduction of Fe in the reducing atmosphere for x is above 0.1. Thus, the following evaluation of the electrical conductivity in humidified hydrogen was demonstrated only for $(\text{La}_{0.045}\text{Sr}_{0.955})(\text{Zr}_{0.95}\text{Fe}_{0.05})\text{O}_{3-\delta}$. As seen in Fig. 2, the electrical conductivity increased by increasing oxygen partial pressure. Among the possible carriers, such as electron, electron hole, oxide ion and proton, only electron hole can be increased by increasing oxygen partial pressure as will be discussed below. Thus, the major carrier of the oxide is considered to be electron hole in oxygen containing environment.



In humidified hydrogen, a significant **Fig. 2** Total conductivity of $(\text{La}_{0.045}\text{Sr}_{0.955})(\text{Zr}_{0.95}\text{Fe}_{0.05})\text{O}_{3-\delta}$ and $\text{SrZr}_{0.99}\text{Fe}_{0.01}\text{O}_{3-\delta}$ [9].

isotope effect of hydrogen and deuterium on the electrical conductivity was observed for $(\text{La}_{0.045}\text{Sr}_{0.955})(\text{Zr}_{0.95}\text{Fe}_{0.05})\text{O}_{3-\delta}$ as well as $\text{SrZr}_{0.99}\text{Fe}_{0.01}\text{O}_{3-\delta}$ [9]. This suggests that the contribution of the protonic conductivity is significant for both oxides in humidified hydrogen. The electrical conductivity of $(\text{La}_{0.045}\text{Sr}_{0.955})(\text{Zr}_{0.95}\text{Fe}_{0.05})\text{O}_{3-\delta}$ was smaller than that of $\text{SrZr}_{0.99}\text{Fe}_{0.01}\text{O}_{3-\delta}$ by 1 – 1.5 orders of magnitude at 1173 K. Oxygen partial pressure dependence of the electrical conductivities between the above oxides is different between the above oxides. The electrical conductivity of $(\text{La}_{0.045}\text{Sr}_{0.955})(\text{Zr}_{0.95}\text{Fe}_{0.05})\text{O}_{3-\delta}$ was increased by decreasing oxygen partial pressure while that of $\text{SrZr}_{0.99}\text{Fe}_{0.01}\text{O}_{3-\delta}$ was independent of oxygen partial pressure. These results suggest that the oxidation state of Fe in the above oxides are different.

In order to examine the difference of the oxidation state, XANES spectra were taken using the powders annealed in various oxygen partial pressures at 1173 K for $(\text{La}_{0.045}\text{Sr}_{0.955})(\text{Zr}_{0.95}\text{Fe}_{0.05})\text{O}_{3-\delta}$ and $\text{SrZr}_{0.99}\text{Fe}_{0.01}\text{O}_{3-\delta}$ [9] because XANES spectra sensitively reflect the electronic state of the components in oxides. The spectra shift toward higher and lower energies when Fe is oxidized and reduced respectively. Figure 3 compares the Fe *K*-edge XANES spectra of $(\text{La}_{0.045}\text{Sr}_{0.955})(\text{Zr}_{0.95}\text{Fe}_{0.05})\text{O}_{3-\delta}$ and $\text{SrZr}_{0.99}\text{Fe}_{0.01}\text{O}_{3-\delta}$ [9], which were annealed in $\log(p_{\text{O}_2} / \text{atm}) = -0.68, -15.73$ and -19.73 at 1173 K and then quenched to room temperature. The spectrum of Fe_2O_3 powder is also shown in the figure. It was found that the spectra of $(\text{La}_{0.045}\text{Sr}_{0.955})(\text{Zr}_{0.95}\text{Fe}_{0.05})\text{O}_{3-\delta}$ obviously shifted toward lower energy as the annealing oxygen partial pressure decreased contrary to $\text{SrZr}_{0.99}\text{Fe}_{0.01}\text{O}_{3-\delta}$. Considering the above results, it can be concluded that Fe in the former oxide is in the mixed valence state of Fe^{2+} and Fe^{3+} while the one in the latter oxide is fixed to be Fe^{3+} in the oxygen partial pressure range investigated. Thus, oxygen vacancy in $\text{SrZr}_{0.99}\text{Fe}_{0.01}\text{O}_{3-\delta}$ is introduced via the eq. (1). On the other hand, for $(\text{La}_{0.045}\text{Sr}_{0.955})(\text{Zr}_{0.95}\text{Fe}_{0.05})\text{O}_{3-\delta}$, the oxygen vacancy is introduced by the partial reduction of iron-ion. The equilibrium of the oxide with oxygen is expressed as,

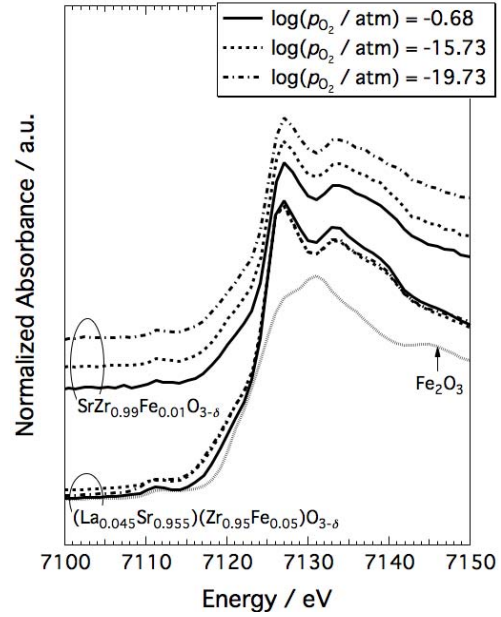


Fig. 3 Normalized Fe *K*-edge XANES spectra of Fe_2O_3 , $\text{SrZr}_{0.99}\text{Fe}_{0.01}\text{O}_{3-\delta}$ [9] and $(\text{La}_{0.045}\text{Sr}_{0.955})(\text{Zr}_{0.95}\text{Fe}_{0.05})\text{O}_{3-\delta}$.

$$V_O^{\bullet\bullet} + \frac{1}{2}O_2 + Fe'_{Zr} = O_O^{\times} + Fe_{Zr}^{\times} + h^{\bullet} \text{ and } K_2 p_{O_2}^{\frac{1}{2}} [V_O^{\bullet\bullet}] [Fe'_{Zr}] = [O_O^{\times}] [Fe_{Zr}^{\times}] [h^{\bullet}] \quad (3)$$

where h^{\bullet} , Fe'_{Zr} and Fe_{Zr}^{\times} are electron hole, Fe^{3+} and Fe^{4+} in Zr-site, respectively. K_2 represents the equilibrium constant. The Fe^{3+} may experience disproportionation into Fe^{2+} and Fe^{4+} [10,11]. Thus, we have,

$$2Fe'_{Zr} = Fe''_{Zr} + Fe_{Zr}^{\times} \text{ and } K_3 [Fe'_{Zr}]^2 = [Fe''_{Zr}] [Fe_{Zr}^{\times}] \quad (4)$$

where K_3 is the equilibrium constant. When the concentration of Fe ions is small such as 0.05, the hopping distance is too long and band conduction becomes predominant. The internal valence of Fe changes due to the trapping of electron hole. One expects,

$$Fe_{Zr}^{\times} = Fe'_{Zr} + h^{\bullet} \text{ and } K_4 [Fe_{Zr}^{\times}] = [Fe'_{Zr}] [h^{\bullet}] \quad (5)$$

where K_4 is the equilibrium constant. The equilibrium of electronic defects,

$$e' + h^{\bullet} = \text{null} \text{ and } K_5 = [e'] [h^{\bullet}] \quad (6)$$

where K_5 is the equilibrium constant. The charge neutrality condition provides,

$$\begin{aligned} [La_{Sr}^{\bullet}] + 2[V_O^{\bullet\bullet}] + [h^{\bullet}] \\ = [Fe'_{Zr}] + 2[Fe''_{Zr}] + [e'] \end{aligned} \quad (7)$$

where $[La_{Sr}^{\bullet}]$ is La^{3+} in Sr^{2+} -site. The site balances of O-site and Fe-site give,

$$[O_O^{\times}] + [V_O^{\bullet\bullet}] = 3 \quad (8)$$

$$[Fe''_{Zr}] + [Fe'_{Zr}] + [Fe_{Zr}^{\times}] = 0.05 \quad (9)$$

Figure 4 (a) shows the Brouwer diagram, which enable to understand the defect concentrations as a function of oxygen partial pressure, of $(La_{0.045}Sr_{0.955})(Zr_{0.95}Fe_{0.05})O_{3-\delta}$ assuming $K_5 \ll K_3 \ll K_4$. In addition, it was also assumed that the concentration of protonic defect is small enough compared to the other positive defects, *i.e.* $[OH_O^{\bullet}] \ll [La_{Sr}^{\bullet}], [V_O^{\bullet\bullet}], [h^{\bullet}]$ for simplicity.

The partial conductivity of species i ,

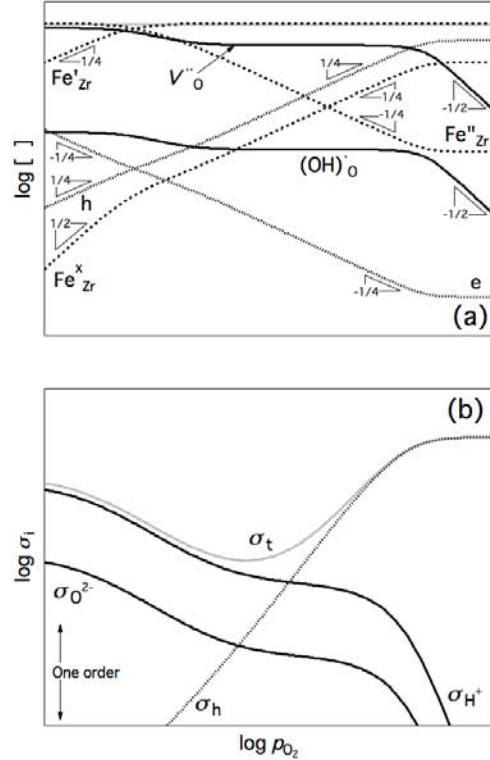


Fig. 4 (a) Brouwer diagram and (b) simulated conductivities as a function of oxygen partial pressure for $(La_{0.045}Sr_{0.955})(Zr_{0.95}Fe_{0.05})O_{3-\delta}$.

σ_i ($i = e, h, O^{2-}$ and H^+), is expressed by,

$$\sigma_i = |z_i| e m_i c_i \quad (10)$$

where z_i , m_i and c_i are charge number, mobility and concentration of species i and e is the elementary charge. When the partial conductivities are assumed to be linear functions of the carrier concentrations, those can be predicted based on the Brouwer diagram constructed as in Fig. 4 (b). Since the contribution of electronic conductivity in the oxide is negligibly small as will be discussed in Section 3.4, thus, the electronic conductivity was not drawn in the figure. Figure 4 (b) shows the simulated conductivities as a function of oxygen partial pressure, assuming $m_{O^{2-}} \ll m_{H^+}$ and $\sigma_e \ll \sigma_h, \sigma_{O^{2-}}, \sigma_{H^+}$. The simulated oxygen partial pressure dependence of the total conductivity is similar to the experimental one as shown in Fig. 2. Thus, the ionic conductivity is predominant in hydrogen containing environment while the electron hole is in oxygen. In this gap of these oxygen partial pressures, the carriers are the mixture of electron hole, oxide ion and protons.

3.4 Evaluation of emf in humidified hydrogen

In order to determine the contribution of partial ionic conductivities in $(La_{0.045}Sr_{0.955})(Zr_{0.95}Fe_{0.05})O_{3-\delta}$, emf measurements were conducted by using hydrogen concentration cells. The theoretical emf value is obtained by,

$$t_{O^{2-}} + t_{H^+} = -\frac{4F}{RT} \frac{\partial E}{\partial \ln p_{O_2}} \quad (11)$$

where $t_{O^{2-}}$ and t_{H^+} , F , R , T , E and p_{O_2} are transport numbers of oxide ion and proton, the Faraday constant, the gas constant, temperature, emf and oxygen partial pressure, respectively. From the neighboring points of the E as a function of p_{O_2} by setting

$$\frac{\partial E}{\partial \ln p_{O_2}} = \frac{\Delta E}{\Delta \ln p_{O_2}} = \frac{(E_{n+1} - E_n)}{(\ln p_{O_2, n+1} - \ln p_{O_2, n})},$$

the transport number of ionic species is evaluated. In humidified environment, it was found that the transport number of ionic species exceeded 0.94 in the temperature range of 973 – 1273 K. The results suggest that the contribution of electronic conductivity is small enough compared to the other species.

3.5 Separation of partial protonic conductivity from the total conductivity

Total conductivity of the oxide is expressed by the sum of partial conductivity

contributions,

$$\sigma = \sigma_h + \sigma_{O^{2-}} + \sigma_{H^+} \quad (12)$$

When the concentration of protonic defect is sufficiently smaller than those of positive defects, *i.e.* oxygen vacancy and La in Sr-site, and the partial conductivities are functions of only carrier concentrations, eq. (12) is rewritten as eq. (13) based on eqs. (2) and (10),

$$\sigma = \sigma_h + \sigma_{O^{2-}} + \sigma_{H^+}^o p_{H_2}^{\frac{1}{2}} \quad (13)$$

where $\sigma_{H^+}^o$ and p_{H_2} are a constant and hydrogen partial pressure, respectively.

Figure 5 shows the total conductivity of $(La_{0.045}Sr_{0.955})(Zr_{0.95}Fe_{0.05})O_{3-\delta}$ typically at 1173 K as a function of square root of water vapor pressure in $\log(p_{O_2} / \text{atm}) = -13.67 \sim -19.70$. It was found that the electrical conductivity is a linear function of the square root of water vapor pressure at temperature shown in Fig. 5. Subtracting the segment values from the total conductivities separates the partial protonic conductivity based on eq. (13). The segment represents the sum of partial conductivity contributions of oxide ion and electron hole, which was shown in Fig. 2.

By the same analysis, the partial protonic conductivity could be separated at 1073 – 1273 K. On the other hand, at 973 K, the electrical conductivity was almost independent of water vapor pressure, suggesting that the separation of the protonic conductivity using eq. (13) is inappropriate at lower temperatures.

3.6 Transport numbers of protons in humidified hydrogen

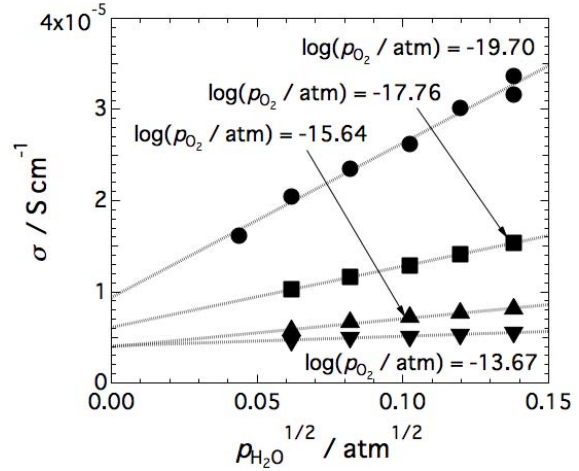


Fig. 5 Total conductivity of $(La_{0.045}Sr_{0.955})(Zr_{0.95}Fe_{0.05})O_{3-\delta}$ as a function of square root of water vapor pressure at 1173 K.

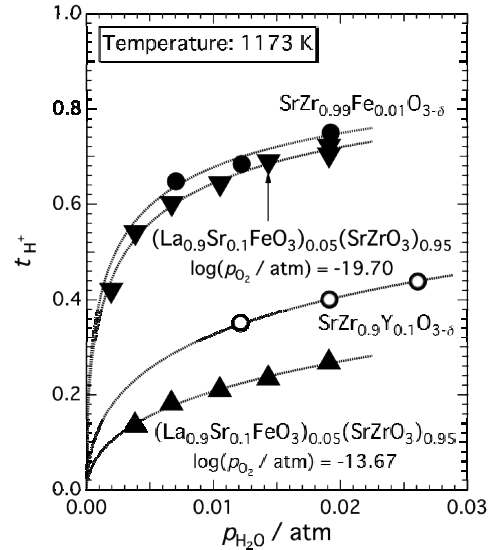


Fig. 6 Transport numbers of protons in various $SrZrO_3$ -based perovskite-type oxides at 1173 K.

Figure 6 compares the transport numbers of protons in various SrZrO₃-based provskite-type oxides, evaluated by Eq. (13), at 1173 K. For (La_{0.045}Sr_{0.955})(Zr_{0.95}Fe_{0.05})O_{3-δ}, it was found that the transport number of proton depended on the oxygen partial pressure. The transport number of proton increased as the oxygen partial pressure decreased. On the other hand, the transport numbers of protons in SrZr_{0.99}Fe_{0.01}O_{3-δ} [9] and SrZr_{0.9}Y_{0.1}O_{3-δ} [12,13] are independent of the oxygen partial pressure. Thus, it can be concluded that the cause of the oxygen partial pressure dependence of the transport numbers of protons essentially comes from the variation of the oxidation state of Fe-ion. For (La_{0.045}Sr_{0.955})(Zr_{0.95}Fe_{0.05})O_{3-δ}, in a lower oxygen partial pressure such as $\log(p_{\text{O}_2} / \text{atm}) = -19.70$, the transport numbers of protons were found to be 0.7 – 0.75, which is comparable with those of SrZr_{0.99}Fe_{0.01}O_{3-δ} [9] and is double of SrZr_{0.9}Y_{0.1}O_{3-δ} [12,13].

4. Conclusions

The defect structure of {La_{0.05(1-x)}Sr_{0.95+0.05x}}(Zr_{0.95}Fe_{0.05})O_{3-δ} ($x = 0, 0.1, 0.25$ and 0.5) was analyzed based on the electrical conductivity, emf and XAS measurements. In oxygen gas, carrier is electron hole for x is below 0.1 while mixture of electron hole, oxide ion and proton for x is above 0.25. In humidified hydrogen for $x = 0.1$, the total conductivity increased by decreasing the oxygen partial pressure due to a variation of oxygen nonstoichiometry caused by the partial reduction of Fe from 3+ to 2+. The transport number of proton was found to increase by decreasing the oxygen partial pressure. This study revealed that the oxides exhibit considerable protonic conductivity. Thus, the ceramic membrane might be applicable to use in hydrogen separation membranes with electrochemical hydrogen pumping.

Acknowledgements

This study was supported by the Technical Research Aid Projects 2010 from the JFE 21st Century Foundation.

References

- [1] F. A. Kröger, H. J. Vink, In: Relations between the Concentrations of Imperfections in Crystalline Solids, F. Steitz and D. Turnbull (Eds.), *Solid State Physics*, Vol.3, Academic, New York (1956).

- [2] H. Iwahara, T. Esaka, H. Uchida, N. Maeda, *Solid State Ionics* **3/4** (1981) 359.
- [3] H. Matsumoto, S. Okada, S. Hashimoto, K. Sasaki, R. Yamamoto, M. Enoki, T. Ishihara, *Ionics* **13** (2007) 93.
- [4] T. Sasamoto, J. Mizusaki, M. Yoshimura, W. R. Cannon, H. K. Bowen, *Yogyo-Kyokai-Shi* **90** (1982) 24.
- [5] J. Mizusaki, W. R. Cannon, H. K. Bowen, *J. Am. Ceram. Soc.* **63** (1980) 391.
- [6] J. Mizusaki, *Solid State Ionics* **52** (1992) 79.
- [7] A. Ahtee, M. Ahtee, A. M. Glazer, A. W. Hewat, *Acta Crystallogr., Sect. B: Struct. Crystallogr. Cryst. Chem.* **32** (1976) 3243.
- [8] A. S. Nowick, A. V. Vaysleyb, *Solid State Ionics* **97** (1997) 17.
- [9] A. Unemoto, A. Kaimai, K. Sato, N. Kitamura, K. Yashiro, H. Matsumoto, J. Mizusaki, T. Kawada, *Solid State Ionics* **181** (2008) 1663.
- [10] J. Mizusaki, M. Yoshimura, S. Yamauchi, K. Fueki, *J. Solid State Chem.* **58** (1985) 257.
- [11] T. Kudo, K. Yashiro, H. Matsumoto, K. Sato, T. Kawada, J. Mizusaki, *Solid State Ionics* **179** (2008) 851.
- [12] K. Yashiro, S. Akoshima, T. Kudo, M. Oishi, H. Matsumoto, K. Sato, T. Kawada, J. Mizusaki, *Solid State Ionics* **192** (2011) 76.